Mechanisms for the NAO Responses to the North Atlantic SST Tripole

SHILING PENG

NOAA–CIRES Climate Diagnostics Center, University of Colorado, Boulder, Colorado

WALTER A. ROBINSON

Department of Atmospheric Sciences, University of Illinois, Urbana, Illinois

SHUANGLIN LI

NOAA–CIRES Climate Diagnostics Center, University of Colorado, Boulder, Colorado

(Manuscript received 10 April 2002, in final form 17 December 2002)

ABSTRACT

The response of an atmospheric general circulation model (GCM) to the North Atlantic SST tripole exhibits both symmetric and asymmetric components with respect to the sign of the SST anomaly. The symmetric part of the response is characterized by a North Atlantic Oscillation (NAO)–like dipole with an equivalent barotropic structure over the Atlantic. The asymmetry is manifested in a weaker and smaller-scale dipole response to the positive SST tripole in contrast to a stronger and more zonally elongated dipole response to the negative tripole. Mechanisms for developing and maintaining these GCM responses are elucidated through diagnostic experiments using a linear baroclinic model and a statistical storm track model based on GCM intrinsic variability.

The NAO-like symmetric response is primarily maintained by a dipolar anomalous eddy forcing that results from interactions between the heating-forced anomalous flow and the Atlantic storm track, as expected from an eddy-feedback mechanism. To account for the asymmetry of the responses about the sign of the SST tripole, a nonlinear eddy-feedback mechanism is proposed that extends the previous mechanism to include the nonlinear self-interaction of the heating-forced anomalous flow and its effects on transient eddy feedbacks. The results of idealized model experiments demonstrate that, due to its nonlinear self-interaction, the tripole heating induces a much weaker response in the positive phase than in the negative phase. Interactions of these nonlinear heating-forced anomalous flows with the Atlantic storm track result in asymmetric eddy vorticity forcings that in turn sustain asymmetric eddy-forced anomalous flows in the two cases.

1. Introduction

One of the most controversial and challenging problems in climate research over recent decades has been to determine the effects of extratropical sea surface temperature (SST) anomalies on the atmosphere and to understand the associated mechanisms (Kushnir et al. 2002). Apart from academic interest, the persistent pursuit of this problem is motivated by two practical considerations. One is the desire to identify oceanic forcing outside of the tropical Pacific that can affect the atmosphere and can potentially be exploited for improving seasonal to interannual forecasts. The other concerns understanding and predicting variability on decadal and multidecadal timescales. Since the atmosphere, on its own, lacks the mechanisms to generate predictable variations on these timescales, potential predictability of such fluctuations can arise only from coupled mechanisms that involve an active ocean. Mechanisms for generating coupled decadal variability in both the North Pacific and the North Atlantic have been proposed (e.g., Latif and Barnett 1994; Cessi 2000; Marshall et al. 2001a; Czaja and Marshall 2001). The validity of these coupled mechanisms depends critically on how the atmosphere responds to extratropical SST anomalies.

Despite the complexity of the problem, significant progress has been made over recent years in understanding the mechanisms determining the atmospheric response to extratropical SST anomalies in atmospheric general circulation models (GCMs) and, by inference, also in nature, as reviewed by Robinson (2000) and Kushnir et al. (2002). Most importantly, the transient-eddy vorticity forcing is identified as playing a critical role in determining the characteristics of the GCM responses (Kushnir and Lau 1992; Ting and Peng 1995; Peng and Whitaker 1999, hereafter PW). The mechanism by which a largely eddy-driven GCM response develops is elucidated by PW using idealized model

Corresponding author address: Dr. Shiling Peng, NOAA–CIRES CDC, R/CDC1, 325 Broadway, Boulder, CO 80305-3328.
E-mail: Shiling.Peng@noaa.gov

experiments. Peng and Whitaker suggested that an extratropical SST anomaly can induce two interacting anomalous forcings: diabatic heating and eddy vorticity forcing. The eddy forcing initially results from interactions between the heating-forced anomalous flow and the storm tracks, but the response to this eddy forcing can, in turn, modify the heating. For example, if the eddy forcing produces a low-level warming above a warm SST anomaly, the anomalous surface heat fluxes will be reduced, or their sign may even be reversed (Latif and Barnett 1994; Peng et al. 1995). The equilibrium GCM response resulting from such interactions between heating and eddy forcing can be strongly eddy driven and characterized by an equivalent barotropic structure, rather than the baroclinic structure associated with the direct response to thermal forcing (e.g., Hoskins and Karoly 1981; Hendon and Hartmann 1982). How effectively the storm tracks are perturbed by the SST anomaly depends on the characteristics of both the SST anomaly and the climatological storm track simulated by the GCM (PW; Walter et al. 2001; Hall et al. 2001). The GCM response to extratropical SST anomalies is, therefore, subject to strong influences from the intrinsic model variability, and it may be model-dependent (e.g., Palmer and Sun 1985; Kushnir and Held 1996; Peng et al. 1997).

The intrinsic model variability affects not only the response near the SST anomaly, but also its hemisphere-wide structure. Extratropical SST anomalies in certain locations can induce hemispheric-scale responses that project strongly on the dominant modes of low-frequency model variability if the latter are hemispherically coherent (Peng and Robinson 2001; Hall et al. 2001). Such SST-induced responses can be largely explained by the shifts in the probability distributions of the dominant modes of intrinsic variability. The internal low-frequency variability in GCMs is known to be mainly eddy driven (Branstator 1992; Ting and Lau 1993). Strong projections of the responses on the dominant modes of variability result when the SST anomaly effectively perturbs the storm tracks and, thus, their associated eddy vorticity fluxes. Recent GCM results reveal that SST-induced responses that project significantly on the dominant model variability have a variance ratio of about 10%–20% on monthly to seasonal timescales (Robinson 2000; Peng and Robinson 2001), thus SST anomalies that are ineffective in perturbing the dominant model variability likely have little detectable impact. This implies that, in nature, SST anomalies that may be optimal in forcing the atmosphere and hence play an active role in generating coupled variability are likely embedded in the SST patterns that are statistically associated with the dominant modes of atmospheric variability.

This consideration led us to conduct the GCM study described in Peng et al. (2002, hereafter PRL) and the current follow-up investigation. PRL showed that, in nature, the hemispherically dominant atmospheric variability during boreal winter, as determined by the leading empirical orthogonal function (EOF) of 500-hPa geopotential heights, comprises a dipole over the Atlantic sector similar to the North Atlantic Oscillation (NAO; Marshall et al. 2001b) and a ridge over the North Pacific. The SST anomalies associated, by simultaneous linear regression, with this leading EOF feature a tripole pattern in the North Atlantic and a positive center in the North Pacific. The North Atlantic SST tripole (see Fig. 1) resembles the anomaly discussed in a number of recent studies indicating its potential influences on the NAO (e.g., Rodwell et al. 1999; Sutton et al. 2000; Czaja and Marshall 2001, Lin and Derome 2003). To determine the robustness of the atmospheric response to this SST tripole and to explore its relationships with the intrinsic model variability, large ensembles of GCM experiments were conducted.

PRL demonstrated that the North Atlantic SST tripole induces a strong NAO-like response only late in the cold season (Feb–Apr), the same period when the model's leading mode of internal variability is most similar to the observed variability and projects strongly on the NAO. The response early in the cold season (Oct–Jan) is much weaker. The SST-induced response in late winter includes not only a NAO-like symmetric component but also an intriguing asymmetric component about the sign of the SST anomaly. Similar asymmetry is identified in observational composites around positive and negative SST tripoles. While the symmetric part of the response may be understood as being generated through the PW eddy-feedback mechanism, this mechanism cannot explicitly account for the asymmetry about the sign of the SST forcing. In this follow-up study, we first examine the maintenance of the GCM responses to the SST tripole and then explore the mechanisms through which they develop. Based on the results of linear model diagnoses, we propose a nonlinear eddy-feedback mechanism that extends the PW mechanism to include the nonlinear self-interaction of the thermally forced response and its effects on transient eddy feedbacks. This mechanism is suggested to be instrumental in inducing the asymmetric GCM responses to the SST tripole.

The paper is organized in five sections. Section 2 describes the GCM and the linear model experiments. Section 3 discusses the maintenance of the GCM responses, and section 4 elucidates the mechanisms. A brief summary and some discussion of the results are provided in section 5.

2. Description of the models and experiments

The results of this study are based on both the GCM and the linear model experiments, as described below.

a. GCM experiments

The GCM used by PRL is a version of the National Centers for Environmental Prediction (NCEP) opera-

tional seasonal forecast model, with a T42 spectral truncation, and 28 vertical levels. Three ensembles of one hundred 8-month (Sep–Apr) runs are conducted using climatological SST and with the SST tripole (Fig. 1) added to or subtracted from the monthly climatology. The 100-member ensemble is formed by initializing the runs with NCEP–National Center for Atmospheric Research (NCAR) reanalysis data of 1–5 September 1980–99. Such large ensembles of runs have rarely been performed in previous studies but are necessary for detecting, with confidence, extratropical SST-forced signals beyond those in the immediate locale of the SST anomaly.

Given a known signal-to-noise ratio (S), the ensemble size (N) required to detect this signal may be roughly estimated, based on the Student's t test [Eq. (14.2.2) in Press et al. 1994], by $N = 2t/S^2$, where t is the Student t value. The variance ratio (S^2) of extratropical SST-induced responses estimated from recent GCM studies is about 10%–20% on monthly to seasonal timescales (Robinson 2000). To detect such a signal at the 95% significance level (i.e., t is about 2), the ensemble size N must be 40–80. A 100-member ensemble allows us to determine any large-scale response with S^2 greater than 8%.

We discuss in the following sections only the GCM response of late winter (Feb–Apr) based mostly on the monthly averaged model output. Filtered daily output are used to calculate the eddy vorticity forcing due to transient perturbations with timescales up to nine days. The filtering is performed by removing from the daily output its low-frequency component, as determined by a 9-day running mean.

b. Linear model experiments

Two linear models are used to diagnose the dynamical maintenance of the GCM response and to understand the underlying mechanisms. One is a dynamical linear baroclinic model (LBM) and the other a statistical storm-track model (STM).

1) DYNAMICAL LBM

The LBM is based on the primitive equations, configured with a T21 horizontal resolution and 10 equally spaced pressure levels. The model is linearized about the GCM February–April basic state averaged over the 100 control runs, or other modified basic states. The maintenance of the GCM response is diagnosed by calculating the LBM response to various GCM anomalous forcings, mainly diabatic heating and eddy vorticity forcing. The LBM must be stable, in the normal mode sense, if it is to produce a stable response to the forcing. This requires the addition of dissipation in the form of Rayleigh friction in the momentum equations and Newtonian cooling in the thermodynamic equation. The timescales for Rayleigh friction and Newtonian damping are 1 day at the lowest level and 7 days above 700 hPa. A biharmonic diffusion with a coefficient of 2×10^{16} $m^4\ s^{-1}$ is applied everywhere, and an additional harmonic thermal diffusion with a coefficient of 2×10^6 $m^2\ s^{-1}$ is included to represent the downgradient heat fluxes by transient eddies. With this dissipation, the LBM takes about 25 days to reach a steady solution. For the sake of examining the effects of various damping rates on the results, the model is run for 60 days for all the experiments.

Simplified dynamical models, such as the LBM, are known to be useful for diagnosing and understanding the GCM responses, but they have certain inherent limitations. For example, the 7-day damping assigned in the free atmosphere to represent the dissipative effects of nonlinear processes is rather arbitrary, and various values have been used in previous studies (e.g., Ting and Hoerling 1993; Ting and Peng 1995). When the damping is decreased (i.e., with a longer timescale), the model produces responses less localized to the forcing with stronger downstream propagation and with increased amplitudes. To simplify the interpretation and comparison of the results, we primarily use a 7-day damping above 700 hPa in the LBM, and the model response is determined by its day-60 solution. A brief comparison with results obtained with a 5-day and a 10-day damping is also shown.

2) STATISTICAL STM

In order to mimic and isolate the GCM eddy feedback processes in a simplified system, one needs to have a STM that can simulate well the GCM storm-track climatology and storm-track perturbations associated with low-frequency circulation anomalies. The STM used by PW is based on the linear quasigeostrophic system forced with Gaussian white noise (Whitaker and Sardeshmukh 1998). This model produces a reasonable climatological storm track over the Pacific, but the simulated Atlantic storm track is flawed, with a tilted axis in the streamfunction-tendency dipole associated with eddy vorticity fluxes, likely due to the limitations of the linear dynamics. In this study, we adopt an alternative approach to simulate the SST-induced eddy feedbacks.

Synoptic-scale eddy variability and low-frequency fluctuations in the atmosphere are known to be interdependent, characterized statistically by a largely linear relationship (e.g., Lau and Nath 1991; Branstator 1992, 1995; Ting and Lau 1993). This suggests that one may construct a statistical STM by determining the relationships between low-frequency circulation anomalies and storm-track variability from a large ensemble of GCM control runs. The statistical STM used in this study is based on the covariance matrix of monthly anomalous heights and monthly streamfunction tendencies due to synoptic eddy vorticity fluxes with timescales up to nine days (hereafter the latter is referred to as eddy vorticity forcing), calculated from a total of 300 months of con-

trol data for February–April. To reduce the noise, the covariance matrix is constructed in EOF space using a certain number of leading height and eddy forcing EOF time series. For convenience, the STM is configured to have a compatible resolution with the LBM. An extended EOF analysis hence is performed using three-dimensional monthly data, on T21 grids and 10 pressure levels over the region north of 20°N, for geopotential height and eddy vorticity forcing. The leading 40 EOFs of each field are retained to construct a normalized covariance matrix ($\mathbf{C}_{yx}$) by normalizing the EOF expansion time series with their respective eigenvalues. The statistical STM in EOF space can simply be expressed as

$$\mathbf{y} = \mathbf{C}_{yx} \cdot \mathbf{x}, \tag{2.1}$$

where vector **x** denotes the predictor field, geopotential height, and vector **y** denotes the predictand field, eddy vorticity forcing. For any given anomalous height field, this STM predicts the eddy forcing based on the covariance matrix $\mathbf{C}_{yx}$ determined from GCM intrinsic variability.

Since SST-forced extratropical responses tend to project strongly on internal variability, as shown later in section 4, this statistical STM can successfully predict the eddy vorticity forcing associated with the tripole SST-forced height response. The pattern correlation between the predicted eddy forcing and the actual forcing calculated from the GCM daily data is as high as 0.9. Such agreement cannot be achieved by the currently known dynamical STMs based on linear dynamics.

We have conducted various STM runs to determine the model sensitivity to the EOF cutoff and found little improvement by including more EOFs. The leading 40 EOFs of geopotential heights explain 94% of the total variance and those of eddy forcing explain 73% of the variance. The statistical STM is used in combination with the LBM in section 4 to explore the mechanisms determining the SST-induced GCM responses. As in PW, the idealized experiments with these simplified models are guided by first examining the relevant GCM forcings, such as diabatic heating and eddy vorticity forcing, associated with the SST-induced circulation response and their relative importance in maintaining the response.

3. Maintenance of the GCM response

Figure 1 displays the SST tripole used in the GCM experiments. It features warm anomalies off the U.S. East Coast flanked by cold anomalies off Newfoundland and in the Tropics. This tripole anomaly is associated, by linear regression, with the leading *hemispheric* mode of atmospheric variability, but it also broadly resembles the SST tripole associated with the NAO and the leading EOF of North Atlantic SST variability (Wallace et al. 1990; Czaja and Frankignoul 2002; Kushnir et al. 2002). The GCM response to the SST tripole and its dynamic maintenance are discussed below.

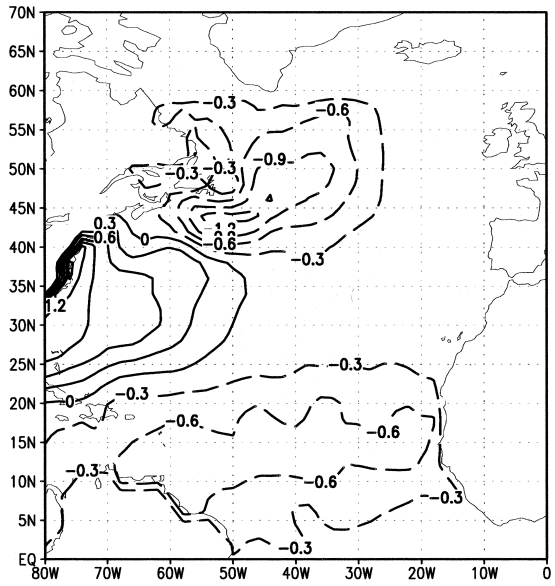

FIG. 1. The tripole SST anomaly (in positive phase) used in the GCM experiments. The contour interval is 0.3 K. In this and succeeding figures, dashed contours are used for negative values.

a. Symmetric response

The GCM response to the SST tripole includes a robust component that is symmetric about the sign of the SST anomaly. This part of the response is determined by the ensemble-mean difference between the runs with positive and negative tripoles. Anomalous geopotential heights at 250 and 850 hPa (Figs. 2a and 2b) are characterized by an equivalent-barotropic NAO-like dipole over the Atlantic sector. The strongest anomalies, near the centers of the dipole, are about 40 m and −50 m at 250 hPa and 20 m and −25 m at 850 hPa. Over the Atlantic, the GCM response strongly resembles observed height regressions on the SST tripole (not shown), capturing up to 40% of the observed regression amplitude. The agreement with the observed regressions is poor over the Pacific.

In nature, the NAO-like anomalous atmospheric circulation can generate the tripole SST anomaly through surface heat flux forcing (e.g., Cayan 1992; Battisti et al. 1995; Marshall et al. 2001b). That the tripole anomaly can, in turn, induce a similar atmospheric response suggests a positive dynamic feedback between the atmosphere and the ocean. Such a positive feedback could orchestrate potentially predictable coupled variability on a range of low-frequency timescales (Czaja and Frankignoul 2002; Czaja and Marshall 2001). To determine the dynamic maintenance of this GCM response to the SST tripole, we next examine the anomalous forcing with which it is associated.

The 950–250-hPa average of the anomalous diabatic heating on T21 grids, computed as the positive minus negative tripole ensemble average, is displayed in Fig. 3. The SST-induced heating exhibits a strong dipole over

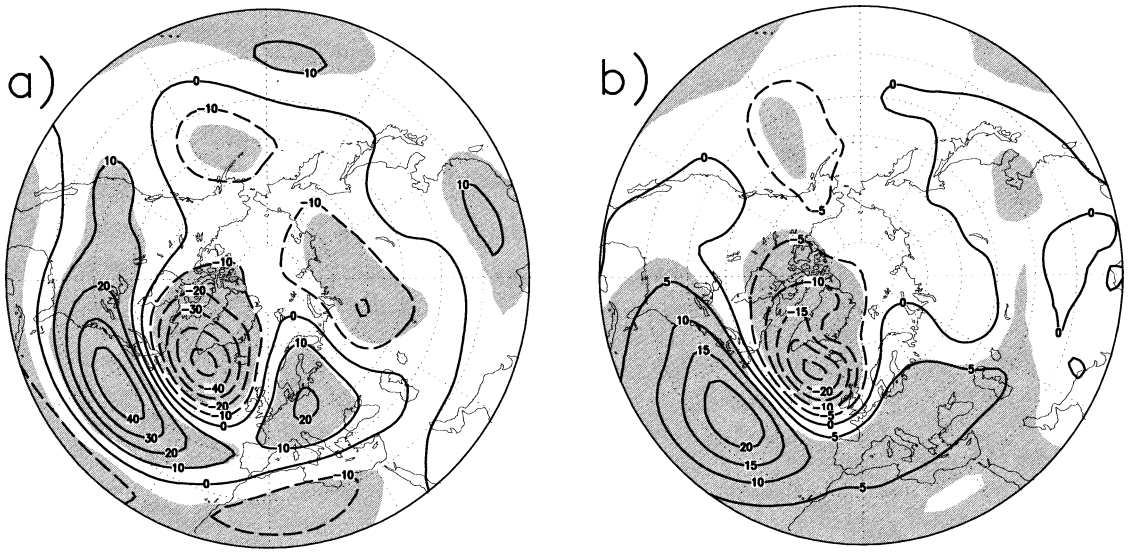

FIG. 2. GCM symmetric geopotential height response at (a) 250 and (b) 850 hPa as the ensemble difference between the runs with positive and negative SST tripoles. Areas with the response significant at the 95% level as estimated by the Student's *t* test are shaded. The contour interval is 10 m in (a) and 5 m in (b).

the mouth of the Amazon (with a maximum cooling of -1.6 K day^{-1}) extending into the eastern Pacific. In the Atlantic basin, the anomalous heating does not closely resemble the pattern of the SST anomaly. North of 50°N positive heating overlies negative SST anomalies, suggesting the potential for a positive thermal feedback of the atmospheric response on the SST anomaly. This is consistent with the sign reversal in the corresponding anomalous surface heat fluxes in this region shown in PRL. The anomalous heating associated with the GCM response is more complex than a simple thermal damping of the SST anomaly, as discussed by Barsugli and Battisti (1998). The heating is strongly modulated by the atmosphere's dynamic response to the SST anomaly.

The rainfall response (not shown) mirrors the heating anomaly shown in Fig. 3. The anomalous heating dipole over the tropical Atlantic is related to a slight southward shift in the climatological rainfall, likely due to the low-level anomalous northeasterlies over the region. LBM experiments forced with GCM anomalous heating in different regions suggest that the tropical heating anomaly, though prominent, plays only a secondary role in maintaining the equilibrium extratropical NAO response.

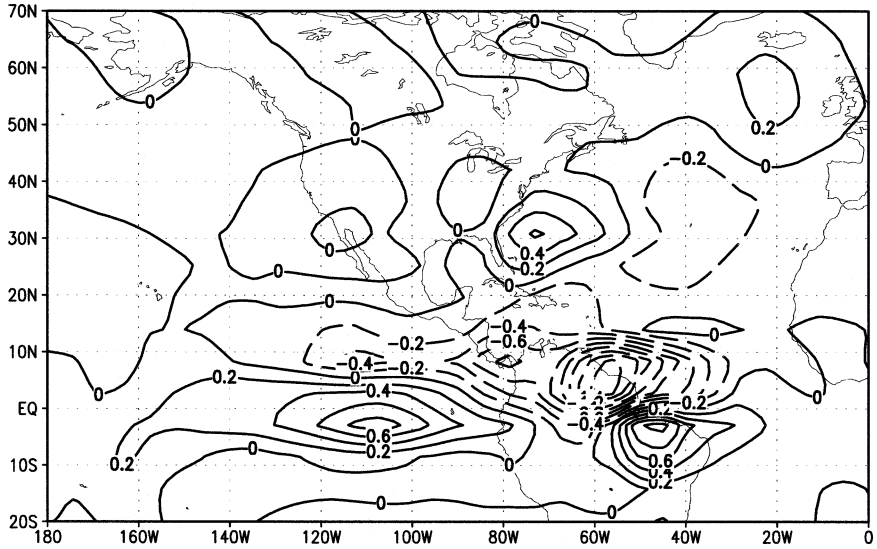

FIG. 3. As in Fig. 2 but for the response in 950–250-hPa averaged diabatic heating. Contour interval is 0.2 K day^{-1}.

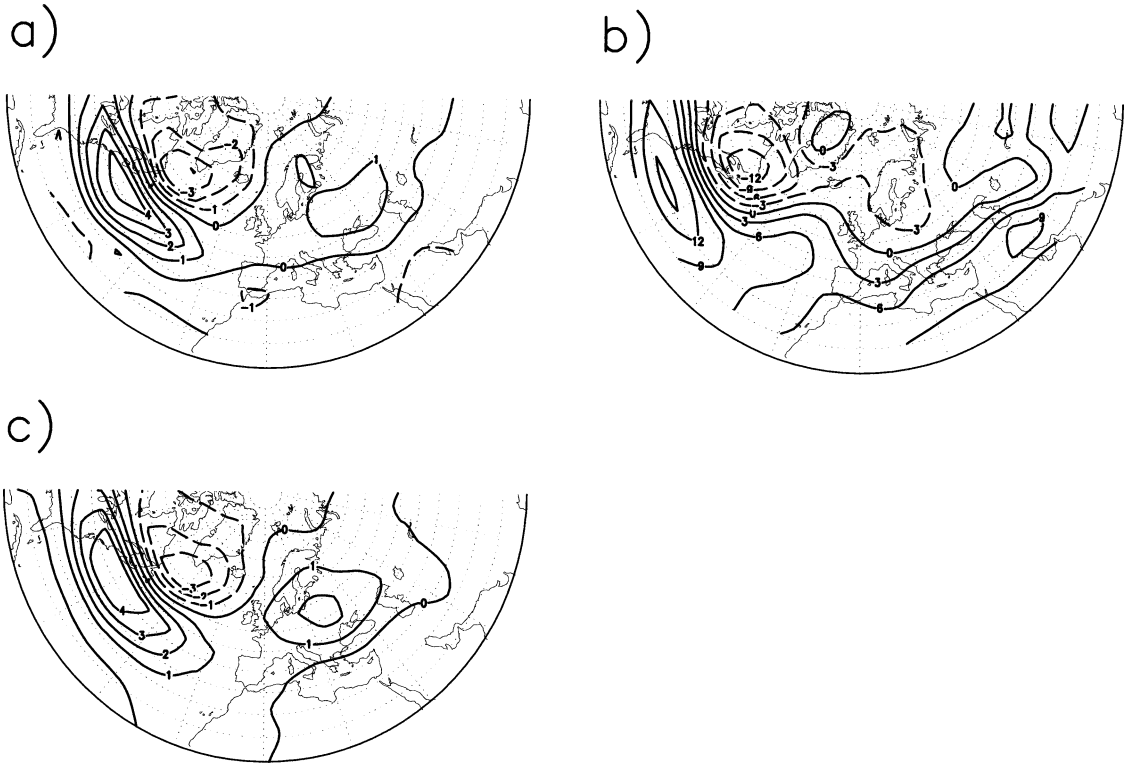

FIG. 4. (a) As in Fig. 2 but for the GCM response in 950–250-hPa averaged streamfunction tendency due to eddy vorticity forcing, calculated from nondivergent winds associated with synoptic eddies. (b) Similar to (a) but for the climatological streamfunction tendency averaged over the control runs. (c) Same eddy forcing as (a) but predicted by the statistical STM from the GCM height response. The contour interval is 1 $m^2\ s^{-2}$ in (a) and (c) and 3 $m^2\ s^{-2}$ in (b).

The anomalous eddy forcing associated with the GCM response is computed as the ensemble-mean difference in the vorticity fluxes due to transient eddies, with timescales up to nine days, calculated from the rotational winds. The anomalous streamfunction tendency on T21 grids corresponding to these eddy vorticity fluxes is depicted in Fig. 4a as its 950–250-hPa average (the maximum at 250 hPa is about 10 $m^2\ s^{-2}$), and for comparison the climatological streamfunction tendency from the 100 control runs is shown in Fig. 4b. The anomalous eddy vorticity forcing features a dipole over the western Atlantic that reinforces the climatological eddy forcing in accelerating zonal winds near 50°N. The strong resemblance between the eddy forcing and the height response (Fig. 2), along with the equivalent-barotropic nature of the latter, suggests that the height response is mainly eddy driven. The contributions that these different GCM forcings make to maintaining the response to the SST anomaly are diagnosed below using the LBM.

The LBM experiments are conducted as described in section 2. The linear responses to the anomalous diabatic heating and the eddy forcing (Figs. 3 and 4a) are displayed in Fig. 5. The heating-induced height anomaly (Figs. 5a,b) is a northeastward-propagating wave train at 250 hPa with a baroclinic structure over the Atlantic. This vertical structure results from the combination of a baroclinic response to the local extratropical heating and an equivalent-barotropic response forced remotely by the tropical heating.

The eddy-forced height anomaly (Figs. 5c,d) is an NAO-like north–south dipole, with an equivalent-barotropic structure over the Atlantic that bears a strong resemblance to the GCM response. This suggests that the pattern of the GCM response is largely determined by the eddy-driven anomalous flow. The total LBM response to the heating and the eddy forcing (Figs. 5e,f) also bears a reasonable spatial resemblance to the GCM response, but with a much weaker amplitude (~50%) likely due to the limitations of the linear dynamics as well as the differences in the model configurations. The details of the discrepancies between the LBM and the GCM responses are also sensitive to the dissipation in the LBM. As shown in Fig. 6, with a 5-day damping applied to the free atmosphere, the corresponding LBM responses (Figs. 6a,b) are more localized near the forcing with weaker downstream propagation and with further reduced amplitudes. The opposite is true for the results with a 10-day damping applied (Figs. 6c,d). Qualitatively, however, these LBM diagnoses provide a consistent picture for the maintenance of the GCM response. The equilibrium response is primarily sustained by the eddy forcing, but the diabatic heating plays a role in shaping its detailed structure. Other

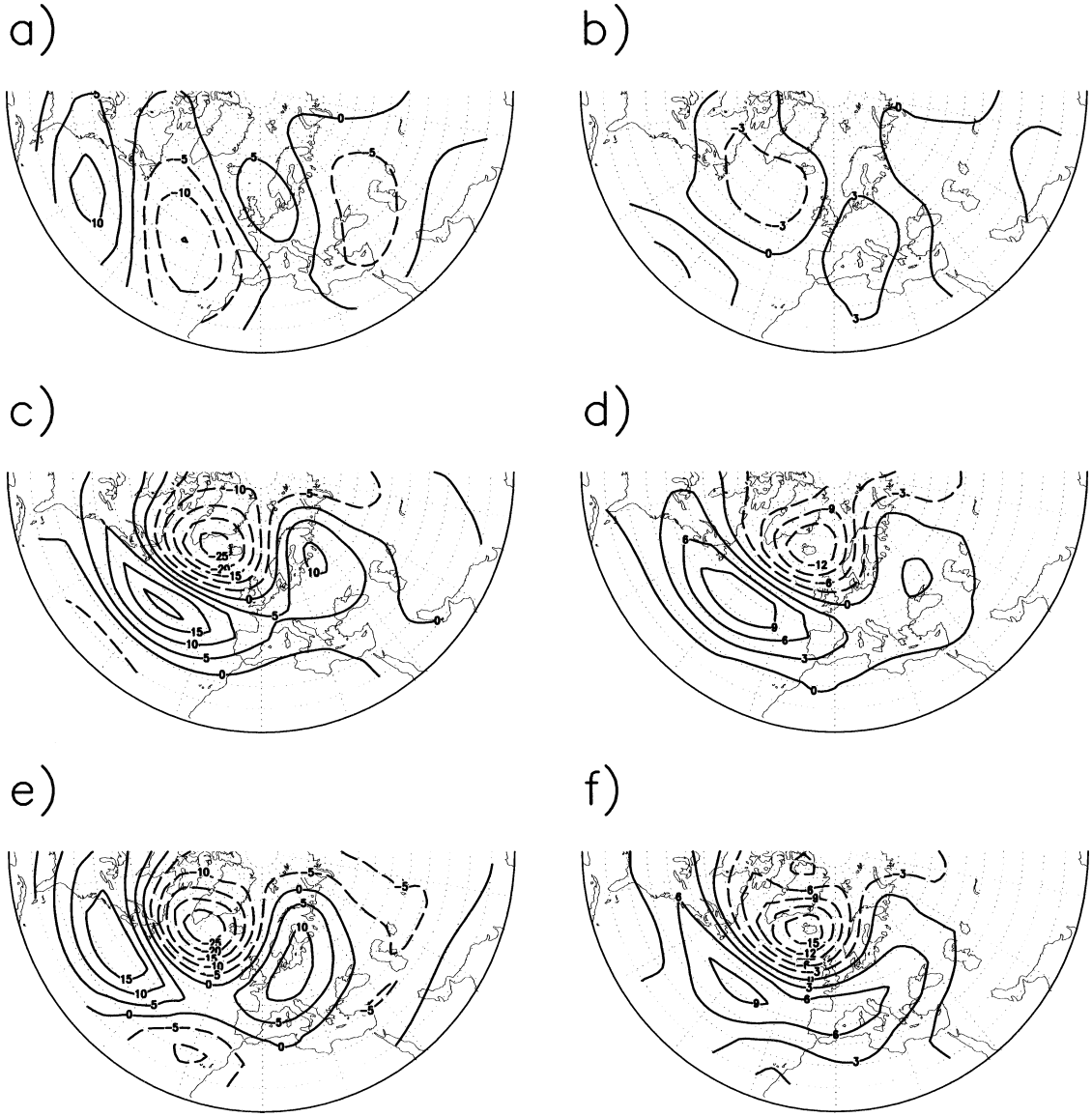

FIG. 5. (a), (b) LBM geopotential height responses at 250 and 850 hPa to the GCM anomalous diabatic heating. (c), (d) As in (a), (b) but for the responses to the anomalous eddy vorticity forcing. (e), (f) The total responses to both the diabatic heating and the eddy forcing. The contour interval is 5 m in (a), (c), and (e), and 3 m in (b), (d), and (f).

forcing terms, such as stationary nonlinearity (i.e., self-nonlinear interaction of the GCM response), are found to be an order of magnitude smaller.

b. Asymmetric response

The separate GCM responses to the positive and the negative SST tripoles are determined as the ensemble-mean differences between the perturbed SST runs and the control runs. As discussed by PRL, the response to the positive tripole is distinctly different from that to the negative tripole, as is shown here in Fig. 7 for the anomalous 250-hPa heights and 850-hPa temperatures. The height anomaly induced by the positive tripole is characterized by a smaller-scale dipole over the western Atlantic with a wave train propagating downstream; the negative tripole induces a more zonally elongated dipole stretching across the Atlantic sector. South of Greenland, the height anomaly induced by the negative tripole (shown here with its sign reversed) is about twice as strong as that induced by the positive tripole. Corresponding to the asymmetric height responses, the anomalous temperatures suggest a greater influence over North America and Siberia by the positive tripole in contrast to a greater influence over Europe and farther south by the negative tripole. This intriguing asymmetry about the sign of the SST tripole is also present in nature, as identified by PRL

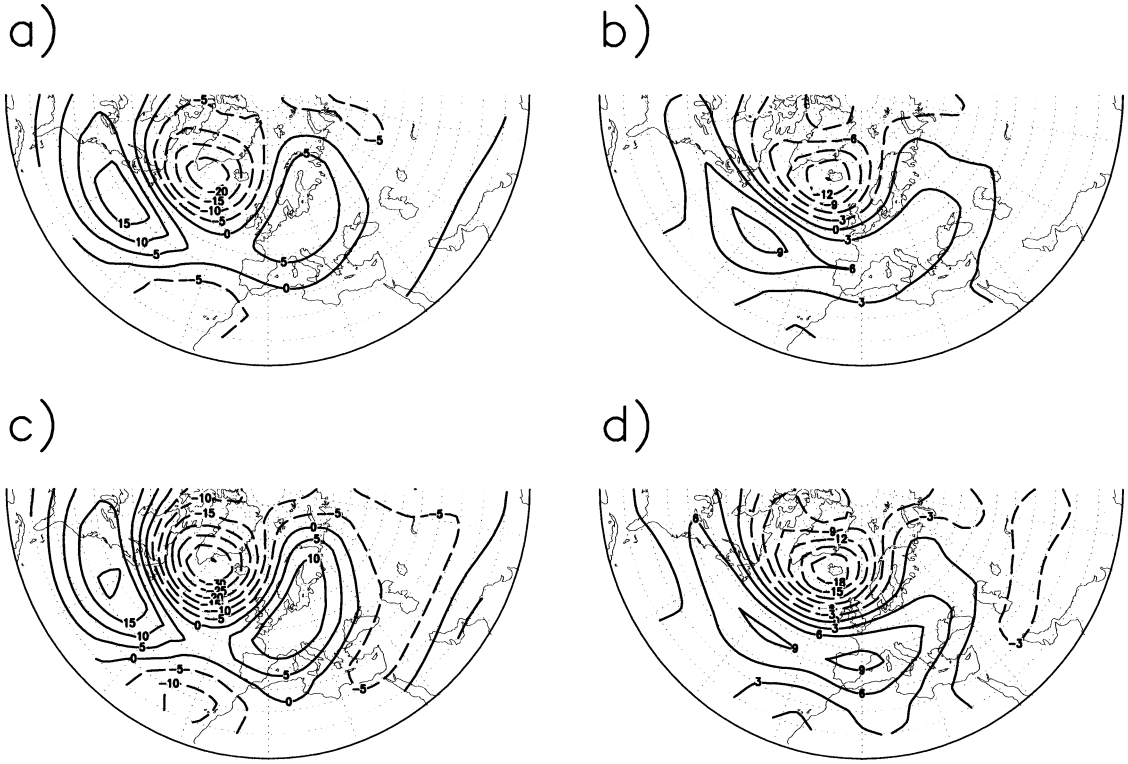

FIG. 6. As in Figs. 5e,f but for the responses with (a), (b) a 5-day damping and (c), (d) a 10-day damping applied above 700 hPa. The contour interval is 5 m in (a) and (c), and 3 m in (b) and (d).

in separate observational composites around positive and negative SST tripoles.

The asymmetric component in the GCM height responses with respect to the sign of the SST tripole is depicted in Fig. 8a as the difference between Fig. 7a and Fig. 7b for the Atlantic sector. The asymmetry is characterized by a positive center over Iceland and a negative center over Europe, reflecting the enhanced and zonally extended NAO response induced by the negative tripole. Like the symmetric response, the asymmetric response is accompanied by a similar asymmetry in the high-frequency eddy forcing (Fig. 8b), although the pattern is noisy. The corresponding asymmetric components in the 850-hPa temperature and the surface heat flux responses are shown in Figs. 8c and 8d. In contrast to the eddy forcing, the sign reversal in the heat flux difference (Fig. 8d) reveals that locally the thermal forcing acts to damp the asymmetric GCM response at equilibrium.

Figure 9 shows the LBM 250-hPa height response to the asymmetric components in both the GCM diabatic heating and the eddy vorticity forcing along with the response to only the asymmetric eddy forcing. Only the eddy forcing over the North Atlantic sector (20°–90°N, 90°W–90°E) is included in these calculations. Despite a weaker signal-to-noise ratio in the asymmetric GCM forcings, the total LBM response (Fig. 9a) exhibits some similarity to the GCM asymmetric response (Fig. 8a) with a positive center near Iceland surrounded by negative anomalies. The negative center north of Iberia in the GCM response is, however, absent from the LBM result. The similarity between Figs. 9a and 9b further suggests that the asymmetric component in the GCM equilibrium responses is largely eddy driven. This confirms again the strong interdependence between the time-mean response and the transient eddy forcing, but it offers no clue as to the origin of the asymmetry. We explore next the mechanisms that can induce the symmetric and asymmetric responses to the SST tripole in GCMs and potentially in nature.

4. Mechanisms for the GCM response

a. Symmetric response

The dynamical maintenance of the symmetric part of the GCM response to the SST tripole as revealed in section 3 is consistent with the PW eddy-feedback mechanism. This suggests that the response develops as follows: the SST tripole initially induces an anomalous heating (Q), which drives a heating-forced anomalous flow (Ψ_H); the latter interacts with the storm tracks resulting in a dipolar anomalous eddy vorticity forcing (F_E); the eddy forcing drives an eddy-forced NAO-like anomalous flow (Ψ_E), which in turn can modify the heating. The *initial*

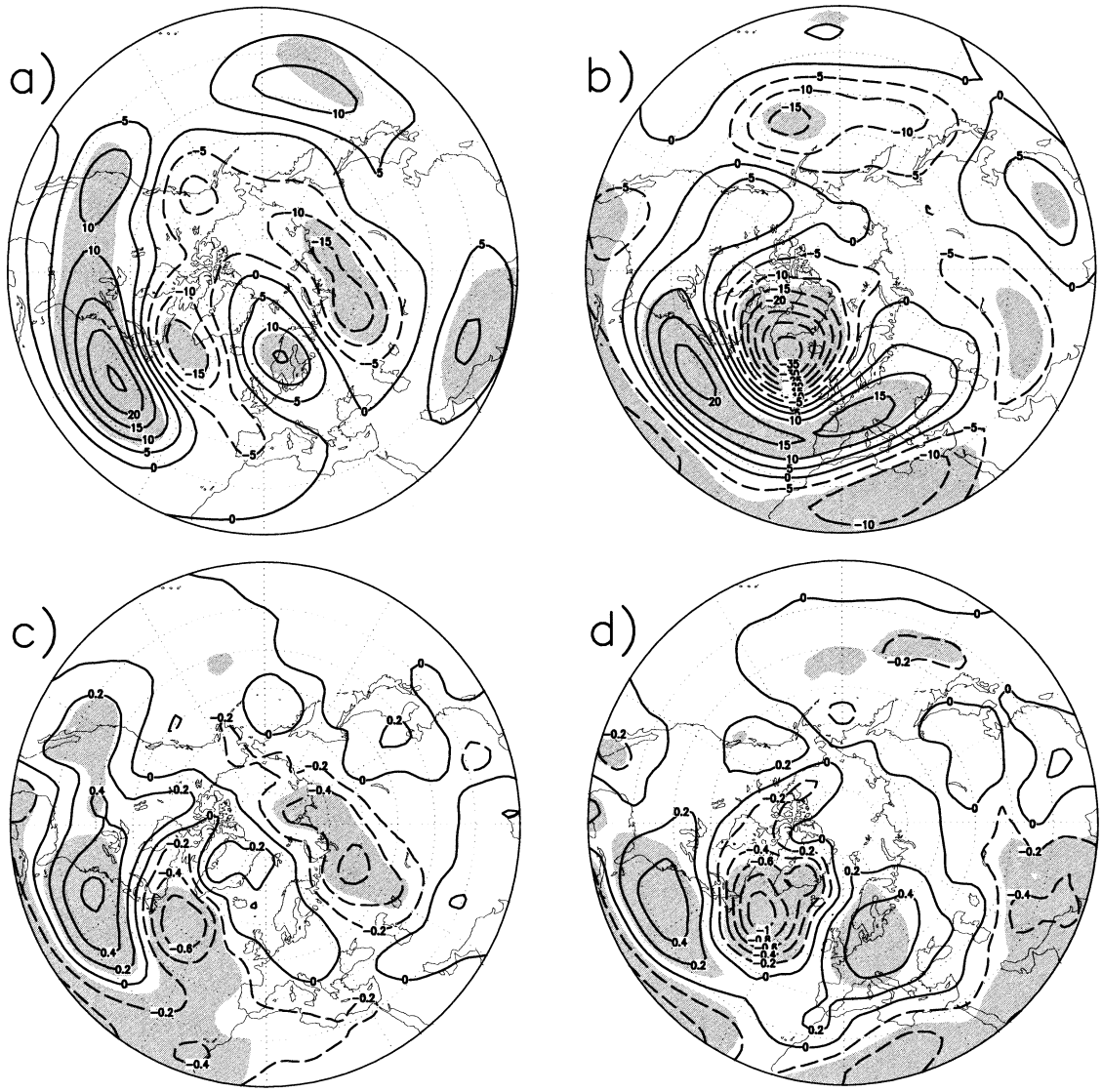

FIG. 7. (a), (b) GCM 250-hPa geopotential height responses to the positive and the negative SST tripoles, as the ensemble difference between the perturbed SST and the control runs. For comparison, the sign in (b) is reversed. Areas with the response significant at the 95% level are shaded. (c), (d) As in (a), (b) but for the 850-hPa temperature responses. The contour interval is 5 m in (a), (b) and 0.2 K in (c), (d).

process of this eddy-feedback mechanism may be summarized by the following schematic:

$$\text{SSTA} \rightarrow Q \rightarrow \Psi_H \rightarrow F_E \rightarrow \Psi_E \qquad (4.1)$$

As illustrated by PW, this process can be simulated with three idealized experiments using the LBM and the STM in combination. First, the LBM is used to determine the heating-forced anomalous flow (i.e., $Q \rightarrow \Psi_H$); second, the STM is used to determine the anomalous eddy forcing (i.e., $\Psi_H \rightarrow F_E$); last, the LBM is used again to determine the eddy-forced anomalous flow (i.e., $F_E \rightarrow \Psi_E$). These idealized experiments are conducted below to determine if indeed the tripole SST can induce a NAO-like response through the PW eddy-feedback mechanism.

The anomalous diabatic heating (Fig. 3) associated with the equilibrium GCM response no longer resembles the SST anomaly because it is modified by the relatively strong eddy-forced response. Before the atmosphere has fully adjusted to the SST anomaly, the anomalous heating should be stronger and roughly proportional to the initial anomalous air–sea temperature difference (i.e., the SST anomaly). Because the dynamic response in early winter (Oct–Jan) is much weaker, the associated anomalous heating is less modified and largely resembles the tripole SST pattern, especially in the lower

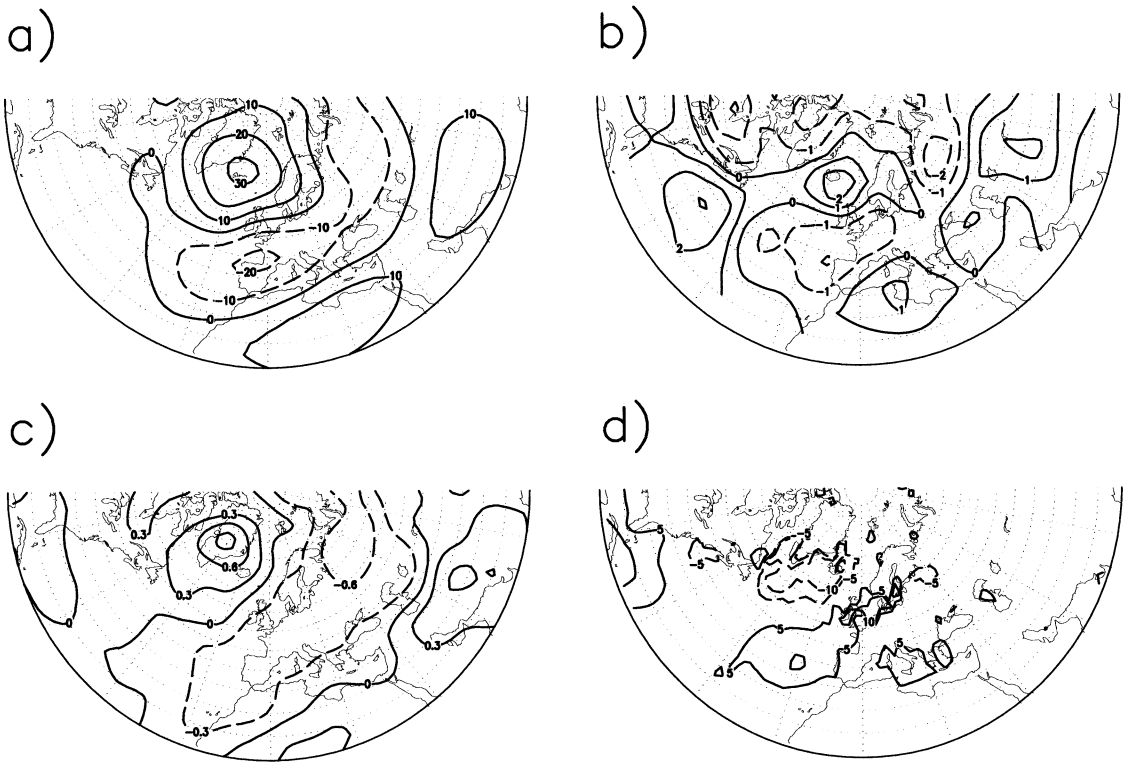

FIG. 8. (a) The asymmetric part of the height responses determined as the difference between Figs. 7a and 7b. (b) Same as in (a) but for the 950–250-hPa averaged eddy vorticity forcing in streamfunction tendency, similar to Fig. 4a. (c) The temperature difference between Figs. 7c and 7d. (d) As in (c) but for the anomalous surface sensible and latent heat fluxes. The contour interval is 10 m in (a), 1 $m^2 s^{-2}$ in (b), 0.3 K in (c), and 5 W m^{-2} in (d). For clarity, zero line is omitted in (d).

troposphere. An idealized *initial* anomalous heating induced by the tripole SST is hence estimated as shown in Fig. 10a. The pattern is extracted from the 950–750-hPa averaged heating anomaly associated with the early winter response. The amplitude of the initial anomalous heating is estimated to be 3 times as strong as the equilibrium heating anomaly, based on the fact that the anomalous air–sea temperature difference at equilibrium has been reduced to roughly one-third of the SST anomaly. A shallow vertical profile is assigned to the heating center off Newfoundland and a deeper profile assigned to the two centers at 15° and 30°N (Fig. 10b), following the GCM heating distributions (see Fig. 10c). Note in Fig. 10a that although the anomalous SST center at 15°N is weakest, it induces the strongest thermal forcing, whereas the SST-induced heating off Newfoundland is weakest. This again implies that extratropical SST anomalies only influence the atmosphere effectively by

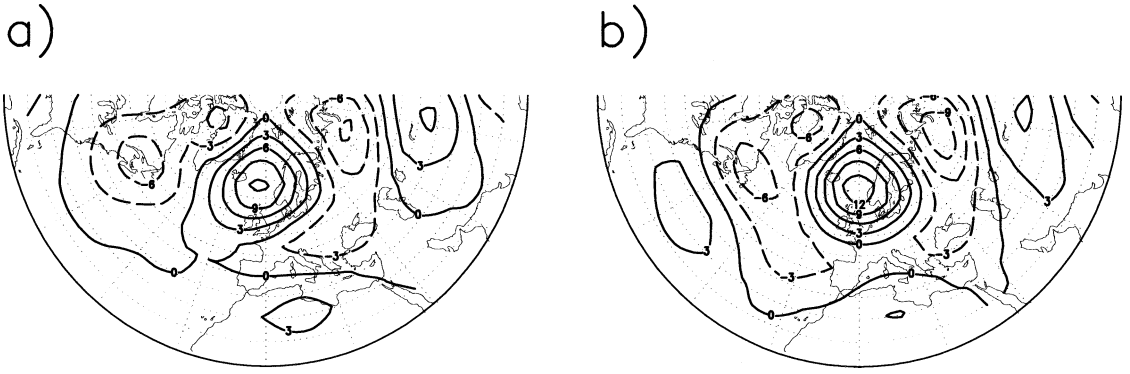

FIG. 9. (a) LBM 250-hPa height response to the asymmetric components in the GCM anomalous heating and the eddy vorticity forcing over the Atlantic sector. (b) Similar to (a) but for the response to the eddy forcing only. The contour interval is 3 m.

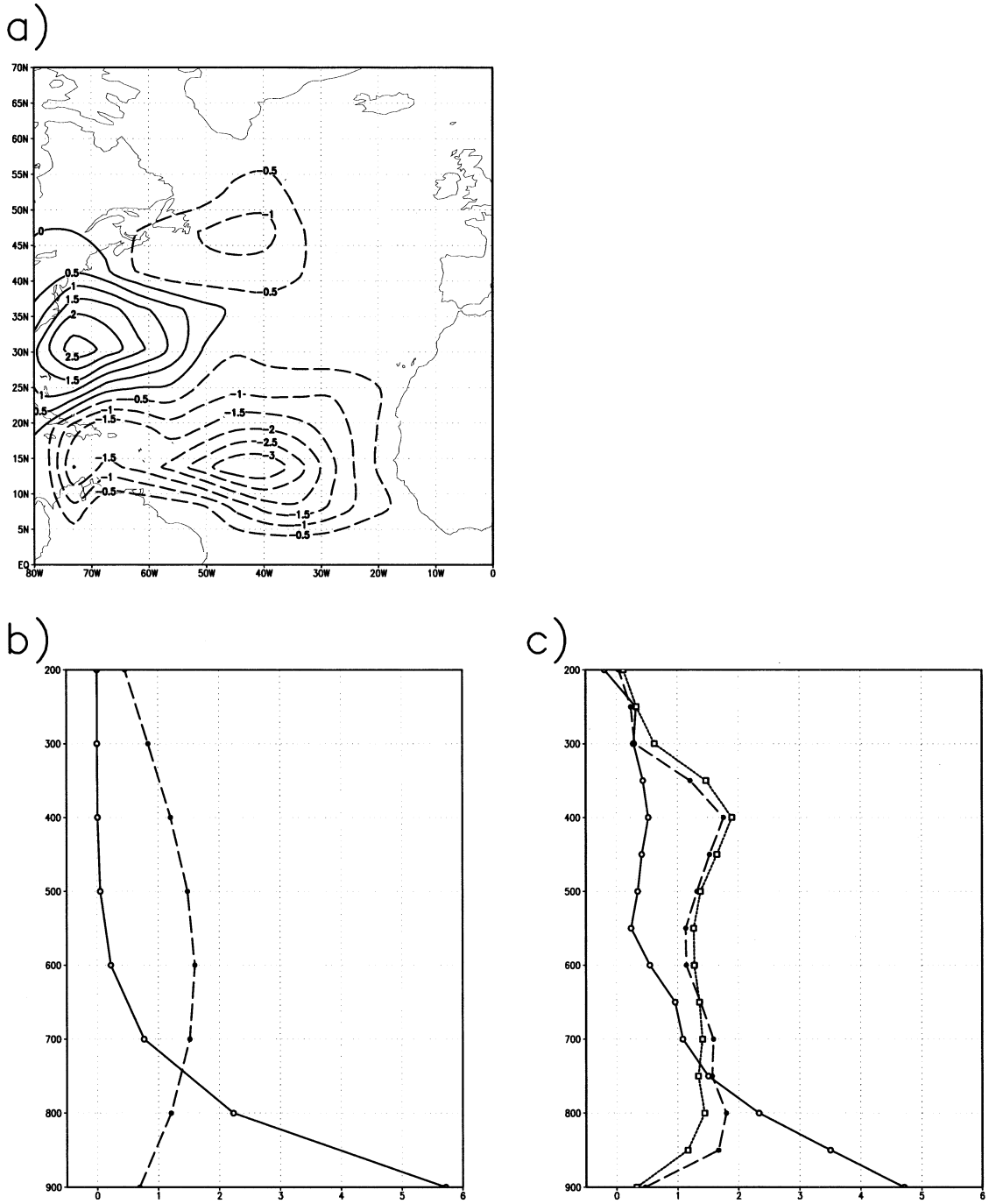

FIG. 10. (a), (b) Idealized initial heating pattern with depth-averaged heating rates, and the vertical heating profiles for the center at 45°N (solid) and for the rest (dash). (c) Similar to (b) but for the GCM heating profiles at 45°N, 50°W (solid); 30°N, 70°W (long dash); and at 15°N, 40°W (short dash). The contour interval in (a) is 0.5 K day^{-1}.

perturbing the storm tracks, rather than through direct thermal forcing.

The tripole heating-forced anomalous flow determined by the LBM (Figs. 11a,b) is characterized by a northeastward-propagating wave train at 250 hPa with a baroclinic structure. The vertical structure of this thermally forced height response is clearly different from the SST-induced GCM response (Fig. 2). The upper-level direct response to the heating bears a certain resemblance to the GCM response but also with noticeable differences. In particular, the SST-induced height response over the Atlantic is a NAO-like north–south dipole whereas the heating-forced dipole is more northeast–southwest oriented. We examine next how the heat-

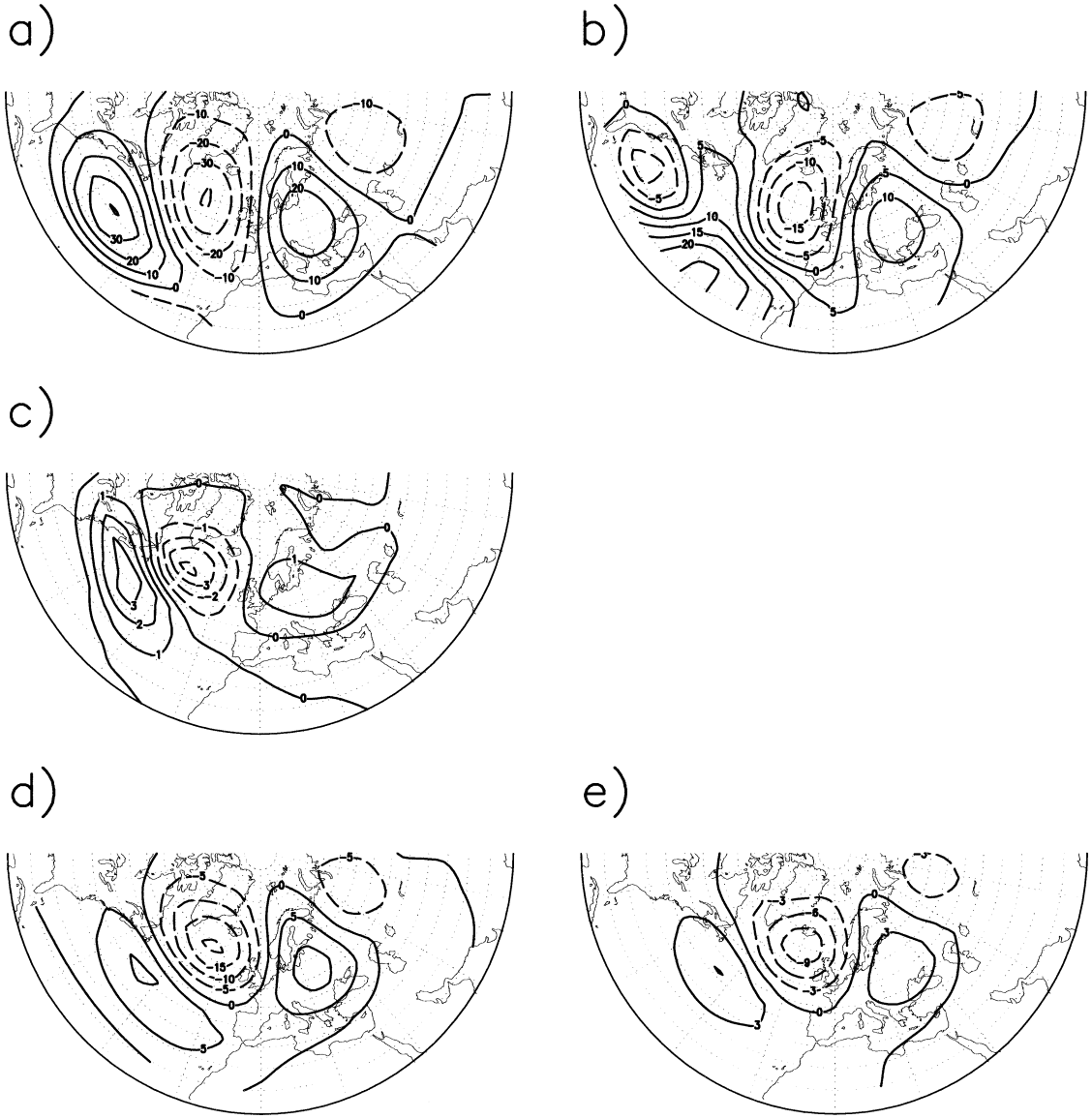

FIG. 11. (a), (b) LBM 250- and 850-hPa geopotential height responses to the idealized heating. (c) The 950–250-hPa averaged eddy vorticity forcing in streamfunction tendency predicted from the heating-forced height response. (d), (e) LBM 250- and 850-hPa geopotential height responses to the eddy forcing. The contour interval is 10 m in (a), 5 m in (b), 1 $m^2\ s^{-2}$ in (c), 5 m in (d), 3 m in (e).

ing-forced anomalous flow interacts with the Atlantic storm track and may be modified by eddy feedbacks.

Before we use the STM to predict the eddy vorticity forcing from the heating-forced anomalous flow, we examine the validity of the model by using it to predict the eddy forcing from the SST-induced GCM height response (Fig. 2). As shown in Fig. 4c the predicted eddy vorticity forcing bears a strong resemblance to the forcing calculated from the GCM daily data (Fig. 4a), with a pattern correlation of 0.9 for the depth-averaged forcing. This agreement suggests that the statistical STM based on GCM intrinsic variability captures the essence of the relationships between the forced anomalous flows and storm track perturbations.

The STM is now used to predict the eddy forcing from the heating-induced height response (Figs. 11a,b) due to its interaction with the Atlantic storm track. The resulting depth-averaged eddy forcing (Fig. 11c) features a dipole pattern over the Atlantic (with a maximum at 250 hPa about 8 $m^2\ s^{-2}$) and a secondary positive center over Europe. The resemblance between this simulated eddy forcing and that from the GCM (Fig. 4a) confirms that the dipolar eddy forcing associated with the GCM response can indeed be induced by the heat-

ing-forced anomalous flow as expected from the PW mechanism. The simulated eddy forcing over the Atlantic sector (20°–90°N, 90°W–90°E) is subsequently used to force the LBM. In comparison with the direct heating-forced response, the eddy-forced anomalous flow (Figs. 11d,e) exhibits a stronger similarity to the GCM response (Fig. 2) in terms of both the vertical structure and the orientation of the Atlantic dipole.

Together the results of the LBM and STM experiments demonstrate that the NAO-like symmetric response to the SST tripole can develop through the PW eddy-feedback mechanism. These experiments are idealized to simulate the initial development of the response in discrete steps in order to separate the heating- and eddy-forced components. In reality, the heating- and eddy-forced anomalous flows interact continuously, and these interactions determine the full GCM response depicted in Fig. 2. Once established, the eddy forcing and the eddy-forced anomalous flow can maintain each other, as they do in the model's internal variability (Branstator 1992, 1995). The eddy-driven flow modifies and weakens the heating, thus becoming more dominant in the equilibrium response.

b. Asymmetric response

The PW eddy-feedback mechanism outlined in (4.1) cannot, however, explain the asymmetry in the GCM responses about the sign of the SST anomaly. To do so, additional interactions must be considered, such as the nonlinear self-interactions of the heating- or eddy-forced anomalous flows and the nonlinear interactions between the heating- and eddy-forced components. We examine below the nonlinear self-interaction of the heating-forced response and its influence on the eddy feedback.

While it is possible that the SST tripole induces asymmetric heating and consequently leads to asymmetric responses about the sign of the SST anomaly, we find that the asymmetry in the SST-induced diabatic heating is small and cannot account for the asymmetric circulation responses. If the diabatic heating initially induced by the SST tripole is symmetric (i.e., equal and opposite in the positive and the negative cases), the asymmetric responses to the heating can also arise from the nonlinear self-interaction of the response. Such heating-forced asymmetric responses (denoted as Ψ_{+Q} and Ψ_{-Q}) may be expressed as

$$\Psi_{+Q} = \Psi_H + \Psi_{\rm NL} \tag{4.2}$$

$$\Psi_{-Q} = -\Psi_H + \Psi_{\rm NL} \quad \text{or} \quad -\Psi_{-Q} = \Psi_H - \Psi_{\rm NL}, \tag{4.3}$$

where Ψ_H denotes the heating-induced linear response under the control basic state (i.e., Figs. 11a,b), and $\Psi_{\rm NL}$ denotes the nonlinear component due to self-interaction of Ψ_H. Note that, since the nonlinearities are quadratic, $\Psi_{\rm NL}$ does not change its sign with the sign of the SST anomaly. The nonlinear component $\Psi_{\rm NL}$ can be obtained by calculating the LBM response under the control basic state to the various forcing terms resulting from Ψ_H self-interaction. Alternatively, when Ψ_H is weak, the asymmetric responses (Ψ_{+Q} and $-\Psi_{-Q}$) can be approximated by calculating the LBM responses to the same heating but with the control basic state modified respectively by ($\Psi_H/2$) and ($-\Psi_H/2$). This approximation can be illustrated by considering, for example, the vorticity flux terms in the LBM associated with a steady response to the heating as follows.

Under the control basic state, Ψ_C, the linearized vorticity fluxes on the right-hand side of the vorticity equation may be expressed as

$$\partial\zeta_H/\partial t = \cdots - (\mathbf{V}_H \cdot \nabla\zeta_C + \mathbf{V}_C \cdot \nabla\zeta_H), \tag{4.4}$$

where ζ is the vorticity, $\mathbf{V}$ is the horizontal vector wind, and $\nabla\zeta$ is the vorticity gradient. The subscript C denotes the control basic state, and the subscript H denotes the heating-forced response. In this case, at equilibrium, the heating-forced response ($\mathbf{V}_H$, ζ_H) corresponds to Ψ_H.

Under the modified basic state, $\Psi_C + \Psi_H/2$, the vorticity fluxes become

$$\partial\zeta_{+Q}/\partial t = \cdots - (\mathbf{V}_{+Q}\cdot\nabla\zeta_C + \mathbf{V}_C\cdot\nabla\zeta_{+Q} + \mathbf{V}_H\cdot\nabla\zeta_H + \text{higher order nonlinearity}). \tag{4.5}$$

In comparison with (4.4), (4.5) now includes an additional vorticity flux ($-\mathbf{V}_H \cdot \nabla\zeta_H$) due to Ψ_H self-interaction. To the extent that higher order nonlinearity is negligible, at equilibrium, the heating-forced response ($\mathbf{V}_{+Q}$, ζ_{+Q}) in (4.5) in effect corresponds to the asymmetric response Ψ_{+Q}. Similarly, for the negative tripole case, $-\Psi_{-Q}$ can be determined from the LBM by modifying the control basic state by ($-\Psi_H/2$).

Figures 12a and 12b show that the asymmetric responses (Ψ_{+Q} and $-\Psi_{-Q}$) to the tripole heating produced by the LBM under the two modified basic states ($\Psi_C + \Psi_H/2$ and $\Psi_C - \Psi_H/2$) are indeed noticeably different. Due to the nonlinear self-interaction, the tripole heating induces a weaker 250-hPa height response in the positive phase (~30 m) than that in the negative phase (~50 m). The difference depicted in Fig. 12c is essentially equal to $2\Psi_{\rm NL}$. It features a positive center (~25 m) over Iceland, similar to that in the GCM response (Fig. 8a), surrounded by negative anomalies. Comparing Figs. 12c and 11a reveals that south of Iceland the amplitude of $\Psi_{\rm NL}$ is about 35% of Ψ_H. Thus the nonlinear component can significantly modify the linear response in the two cases. We suspect that $\Psi_{\rm NL}$ is mainly driven by the barotropic Ψ_H self-interaction (i.e., $-\mathbf{V}_H \cdot \nabla\zeta_H$). This nonlinear vorticity flux is directly calculated from the rotational winds associated with Ψ_H (i.e., Figs. 11a,b), and then used to force the LBM under the control basic state. The doubled 250-hPa height response to this vorticity forcing as shown in Fig. 12d indeed strongly resembles the total nonlinear component in Fig. 12c.

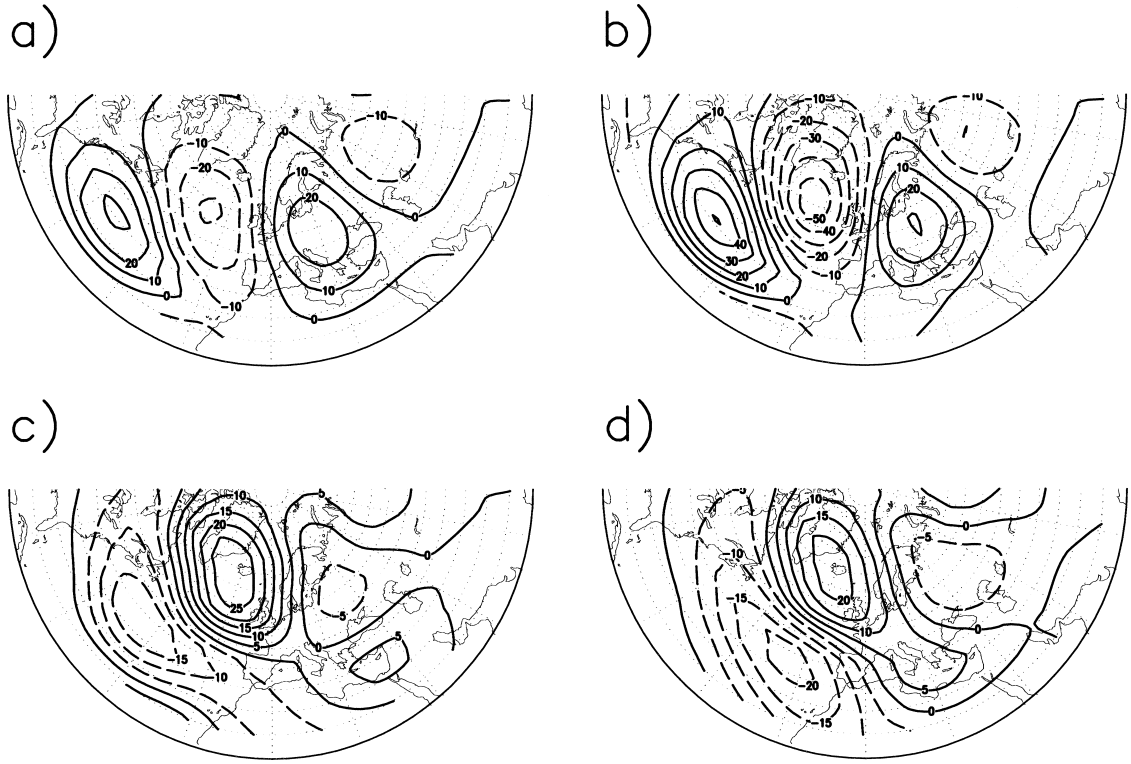

FIG. 12. LBM asymmetric 250-hPa geopotential height responses to the initial heating under the basic states modified to include the nonlinear self-interaction for (a) positive and (b) negative tripole phases. (c) The difference between (a) and (b). (d) The doubled LBM 250-hPa height response under the control basic state to the vorticity flux convergence calculated directly from the heating-forced anomalous flow depicted in Figs. 11a,b. The contour interval is 10 m in (a), (b), and 5 m in (c), (d).

Similar experiments are performed with the LBM forced by different parts of the tripole heating to determine their relative contributions to the nonlinearity in Fig. 12c. About 50% of the nonlinearity arises from the self-interaction of the tropical heating-forced anomaly and the rest from the extratropical dipole heating and the interaction between the tropical and extratropical components. It is intriguing that the nonlinear effects due to these self- and cross-interactions of different parts of the tripole heating act to reinforce rather than cancel each other. This likely contributes to the robustness of the asymmetry in the SST tripole-induced GCM responses. A somewhat similar nonlinearity is detected in a recent GCM study by Kucharski and Molteni (2003) with an Atlantic SST tripole.

While the nonlinear component induced directly by the initial Ψ_H self-interaction bears a resemblance to the GCM asymmetric component over Iceland and to the east, there are noticeable differences. The negative anomalies in Fig. 12c are centered upstream of those in the GCM (Fig. 8a). We examine next how this heating-induced nonlinearity is modified by transient eddy feedbacks and by other nonlinear interactions.

The STM is used to predict the eddy vorticity forcing from the heating-forced asymmetric anomalous flows (Figs. 12a,b). As expected, the heating-induced nonlinearity results in a weaker dipole eddy forcing in the positive tripole case (Fig. 13a) than that in the negative tripole case (Fig. 13b). The LBM responses to these asymmetric eddy forcings under the control basic state are subsequently calculated. Like the eddy-forced symmetric response (Fig. 11d), the eddy-forced asymmetric height responses (Figs. 13c,d) are characterized by a NAO-like north–south dipole stretched across the Atlantic but with considerable amplitude differences between the two cases. The eddy-forced response in the negative tripole case is much stronger and likely determines the more zonally elongated GCM response (Fig. 7b), as the response in the GCM evolves to be more strongly eddy driven. The asymmetric component in these eddy-forced responses, as depicted in Fig. 13e, exhibits a stronger similarity to the GCM nonlinear component (Fig. 8a), with the negative anomalies over the Atlantic shifted slightly downstream of those induced directly by the heating (Fig. 12c). This suggests that through transient eddy feedbacks the nonlinearity initially induced by heating is modified and its structure grows closer to the asymmetry in the GCM equilibrium responses.

Similar to the heating-induced nonlinearity, we also examine the effects of two other nonlinear interactions, namely the self-interaction of eddy-forced anomalous flow and the interaction between the heating- and eddy-forced components, by calculating the LBM responses

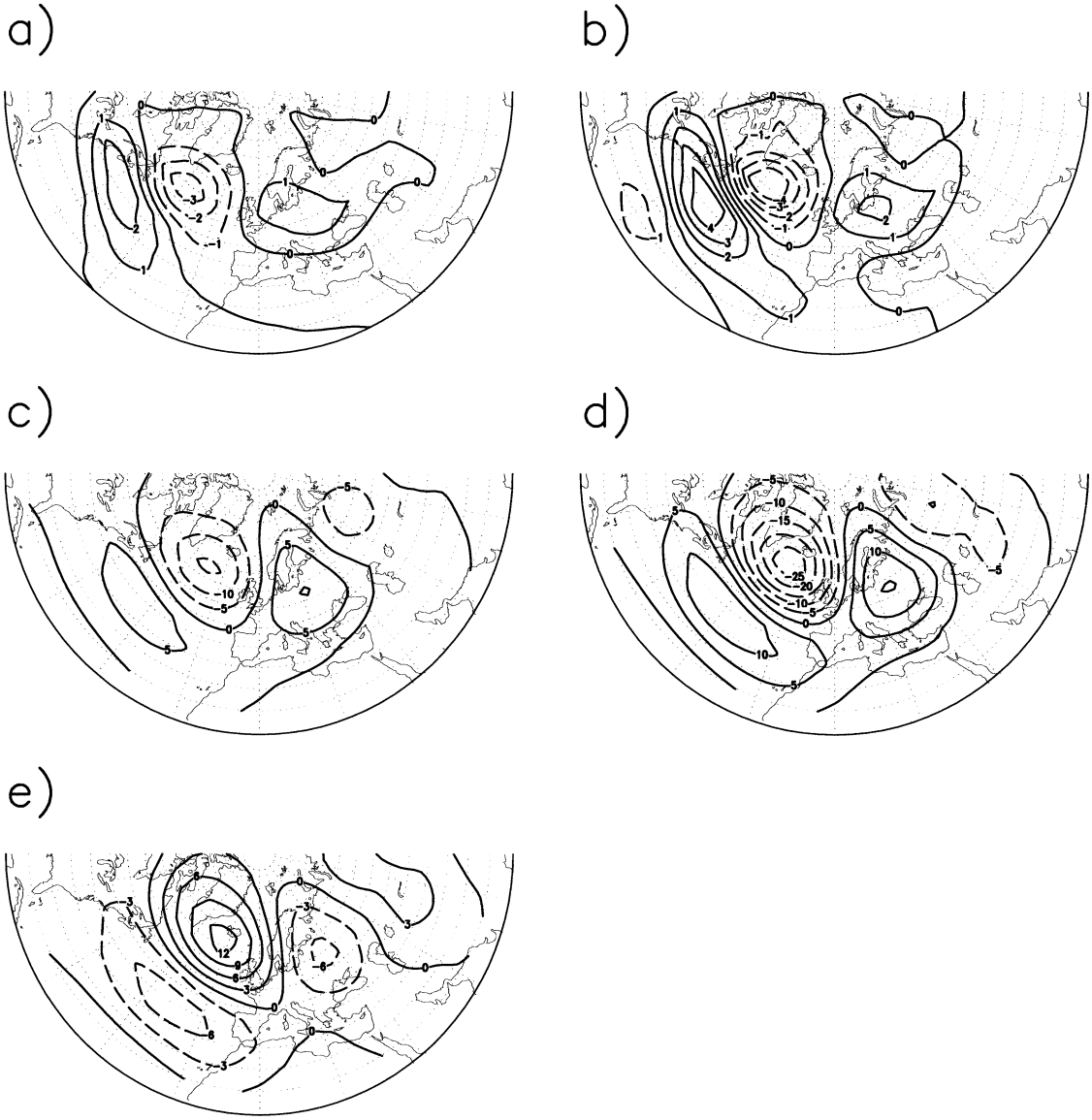

FIG. 13. (a), (b) Asymmetric 950–250-hPa averaged eddy vorticity forcing in streamfunction tendency predicted from the asymmetric heating-forced height responses for positive and negative tripole cases. (c), (d) LBM 250-hPa geopotential height responses to the asymmetric eddy forcing under the control basic state for positive and negative cases. (e) The difference between (c) and (d). The contour interval is 1 $m^2 s^{-2}$ in (a), (b), 5 m in (c), (d), and 3 m in (e).

to the asymmetric eddy forcings under the various modified basic states. These nonlinear effects (not shown) are found to be much weaker in comparison with the self-interaction of the response to heating and play a negligible role in the initial development of the asymmetric responses. It is possible however that, as the responses evolve toward the equilibrium in the GCM, these nonlinear interactions may grow stronger and modify the detailed structure of the eddy-forced asymmetric component.

We suspect that the eddy-forced component (Fig. 9b) in the GCM nonlinear response determined by the LBM is probably obscured by the noise in the GCM asymmetric eddy forcing (Fig. 8b). As for the symmetric eddy forcing, the asymmetric eddy forcing can also be predicted by the STM from the GCM asymmetric height response (Fig. 8a) at all levels. The predicted depth-averaged asymmetric eddy forcing (Fig. 14a) features a much smoother dipole over the eastern Atlantic than that calculated from the GCM daily data. The LBM 250-hPa height response (Fig. 14b) to the predicted eddy forcing bears a clear resemblance to the GCM asymmetric response (Fig. 8a). Moreover, this eddy-forced asymmetric component associated with the GCM response is remarkably similar to that depicted in Fig. 13e. This similarity further suggests that the nonlinearity

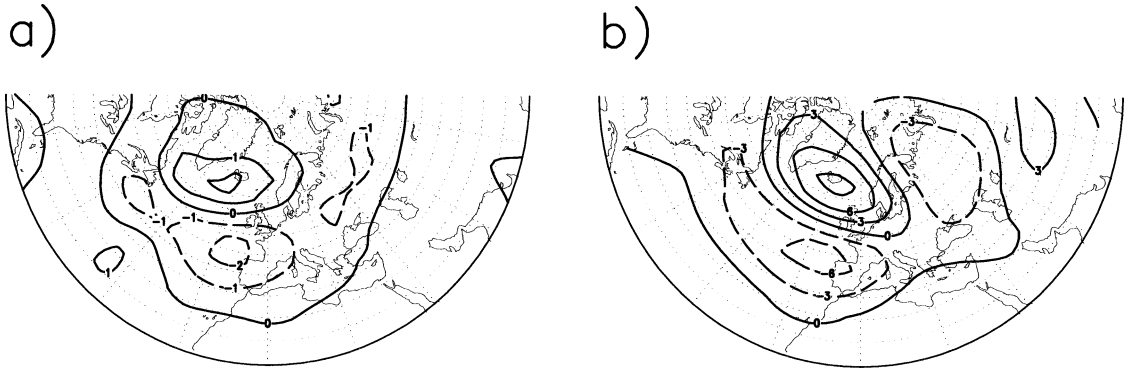

FIG. 14. (a) The 950–250-hPa averaged eddy vorticity forcing in streamfunction tendency predicted from the GCM asymmetric part of the height responses (Fig. 8a). (b) LBM 250-hPa height response to the eddy forcing. The contour interval is 1 $m^2\ s^{-2}$ in (a) and 3 m in (b).

originating from the self-interaction of the heating-forced anomalous flow simulated with the above LBM and STM experiments captures the essence of the asymmetry in the GCM responses.

Considering that the LBM tends to produce much weaker responses to forcing, the full heating as depicted in Fig. 10a is used in simulating the heating-forced asymmetric responses shown in Fig. 12. To determine the sensitivity and robustness of the heating-induced nonlinearity, similar LBM experiments (not shown) are repeated for different damping rates and heating strength. As expected, we found from these experiments that with a weaker damping applied in the free atmosphere, the nonlinearity grows with the strength of the heating-forced response, and vice versa. A largely similar effect results from varying the strength of the heating. These variations, however, have little effect on the spatial pattern of the nonlinearity. The same is found to be true for reasonable variations in the vertical heating profiles.

As in the symmetric case, the simulated initial heating- and eddy-forced asymmetric responses (Figs. 12a,b and 13c,d) and their associated forcings will interact continuously as the responses evolve toward the equilibrium in the GCM. In the process, the SST-induced initial heating can be modified and weakened by the eddy-forced component. As a result, at equilibrium, the asymmetric part of the GCM responses (Fig. 8a) is largely eddy-driven. As illustrated above, the asymmetry in the equilibrium eddy forcing likely stems from the nonlinear self-interaction of the initial heating-forced response. We propose, therefore, a nonlinear eddy feedback mechanism by which asymmetric responses to opposite SST anomalies may develop in GCMs, and by inference in nature, as summarized here:

$$\text{SSTA} \rightarrow Q \rightarrow \begin{cases} \rightarrow \Psi_{+Q} \rightarrow F_{+E} \rightarrow \Psi_{+E} \\ \rightarrow \Psi_{-Q} \rightarrow F_{-E} \rightarrow \Psi_{-E} \end{cases} \quad (4.6)$$

The symbols used here are similar to those in (4.1) except that Ψ_{+Q} and Ψ_{-Q} denote the heating-induced asymmetric anomalous flows defined in (4.2) and (4.3) and depicted in Figs. 12a,b (with a sign reversal in Fig. 12b). Similarly, F_{+E} and F_{-E} denote the resulting asymmetric eddy forcings (Figs. 13a,b), and Ψ_{+E} and Ψ_{-E} denote the asymmetric eddy-forced anomalous flows (Figs. 13c,d). Again, this schematic represents the *initial* process for developing the asymmetric responses that originate from the nonlinearity in Ψ_{+Q} and Ψ_{-Q}. The equilibrium GCM responses will be determined by the interactions among these different components as discussed above.

5. Summary and discussion

Large ensembles of GCM experiments were conducted by PRL to determine the atmospheric responses to the North Atlantic SST tripole in its opposite phases. The GCM responses exhibit both symmetric and asymmetric components with respect to the sign of the SST anomaly. The symmetric part of the height responses, defined as the ensemble-mean difference between the runs with the positive and the negative tripoles, is characterized by a NAO-like dipole with an equivalent barotropic structure over the Atlantic. The asymmetry is manifested in a weaker and smaller-scale dipole response over the eastern Atlantic with a downstream wave train to the positive tripole, in contrast to a stronger and more zonally elongated dipole response across the entire Atlantic to the negative tripole. This study investigates the mechanisms for developing and maintaining these GCM responses through LBM and STM experiments, based on GCM and idealized forcings. Unlike in earlier studies (Branstator 1995; PW; Watanabe and Kimoto 2000), the STM used here is a statistical model constructed from the intrinsic variability of the GCM.

Comparing the LBM responses to the different GCM anomalous forcings reveals that the NAO-like GCM symmetric response is primarily sustained by a dipolar anomalous eddy vorticity forcing, resulting from SST-

induced perturbations in the Atlantic storm track. The anomalous diabatic heating modifies the detailed structure of the GCM response. Similarly, the asymmetric part of the GCM responses is also largely eddy-driven at equilibrium. To determine if the NAO-like symmetric response may develop in the GCM through the eddy-feedback mechanism described by PW, the anomalous flow induced by an idealized initial tripole heating and its interaction with the Atlantic storm track are simulated with the LBM and STM. Consistent with the PW mechanism, the results of these experiments suggest that the NAO-like height response results from transient-eddy modulations of an initially tripole-heating-forced anomalous flow.

To account for the asymmetry in the GCM responses about the sign of the SST anomaly, the PW, mechanism is extended to include the nonlinear self-interaction of the heating-forced anomalous flow and its effects on transient-eddy feedbacks. Results from LBM experiments demonstrate that, with the effect of nonlinear self-interaction included, the tripole heating induces a much weaker response in the positive tripole case than that in the negative phase. Interactions of these heating-forced asymmetric anomalous flows with the storm track result in asymmetric eddy forcings in the two cases. These asymmetric eddy forcings in turn produce asymmetric eddy-forced anomalous flows. Through transient-eddy feedbacks the nonlinearity originally induced by the heating is modified, and it becomes more similar to the asymmetric component in the GCM equilibrium responses. The nonlinear self-interaction of the heating-forced anomalous flow is suggested to be the initial cause for the asymmetric responses about the sign of the SST tripole in the GCM.

The LBM and STM experiments in this study are idealized in order to separate the heating- and eddy-forced components and to effectively isolate the origin of the nonlinearity about the sign of the SST anomaly. These experiments are not aimed at reproducing the equilibrated GCM response, but rather to elucidate the underlying mechanisms. It is worth mentioning that the asymmetry induced by the self-interaction of the heating-forced anomalous flow may exert a back influence on the heating and produce an asymmetric component in the heating. Hence, differences in the heating anomalies (and also in the eddy forcing) associated with the GCM asymmetric circulation responses at equilibrium do not necessarily indicate causality.

Apart from enabling the development of asymmetric responses to opposite SST tripoles, the proposed nonlinear eddy-feedback mechanism may generate additional nonlinearity in the SST-induced GCM responses. For example, we find from parallel GCM experiments that the response induced by the full SST tripole is about twice as strong as the sum of the responses induced separately by the extratropical and the subtropical parts of the tripole, consistent with the results of Sutton et al. (2000). How such nonlinearity about the pattern of the SST anomaly is generated and to what extent it may be attributed to the present nonlinear eddy-feedback mechanism remain to be investigated. On a broader scope, further studies are also needed to determine the influences of the tripole SST-induced asymmetric NAO responses on related climate variability, such as the Arctic Oscillation and extratropical coupled atmosphere–ocean variability (Thompson and Wallace 1998; Kimoto et al. 2001).

Acknowledgments. We gratefully acknowledge Dr. Jeffrey S. Whitaker for kindly helping us to construct the statistical STM and for providing us with the LBM. We are also thankful to Dr. Nicholas Hall and an anonymous reviewer for their insightful critiques that led to significant changes and improvements of the manuscript. This research is supported in part by NSF Grants ATM-9902816 and ATM-9903503.

REFERENCES

Barsugli, J. J., and D. S. Battisti, 1998: The basic effects of atmosphere–ocean thermal coupling on midlatitude variability. *J. Atmos. Sci.,* **55,** 477–493.

Battisti, D. S., U. S. Bhatt, and M. A. Alexander, 1995: A modeling study of the interannual variability of the North Atlantic Ocean. *J. Climate,* **8,** 3067–3083.

Branstator, G., 1992: The maintenance of low-frequency atmospheric anomalies. *J. Atmos. Sci.,* **49,** 1924–1945.

——, 1995: Organization of storm track anomalies by recurring low-frequency circulation anomalies. *J. Atmos. Sci.,* **52,** 207–226.

Cayan, D. R., 1992: Latent and sensible heat-flux anomalies over the northern oceans—The connection to monthly atmospheric circulation. *J. Climate,* **5,** 354–369.

Cessi, P., 2000: Thermal feedback on wind stress as a contributing cause of climate variability. *J. Climate,* **13,** 232–244.

Czaja, A., and J. Marshall, 2001: Observations of atmosphere–ocean coupling in the North Atlantic. *Quart. J. Roy. Meteor. Soc.*, **127,** 1893–1916.

——, and C. Frankignoul, 2002: Observed impact of Atlantic SST anomalies on the North Atlantic Oscillation. *J. Climate,* **15,** 606–623.

Hall, N. M. J., J. Derome, and H. Lin, 2001: The extratropical signal generated by a midlatitude SST anomaly. Part I: Sensitivity at equilibrium. *J. Climate,* **14,** 2035–2053.

Hendon, H. H., and D. L. Hartmann, 1982: Stationary waves on a sphere: Sensitivity to thermal feedback. *J. Atmos. Sci.,* **39,** 1906–1920.

Hoskins, B. J., and D. Karoly, 1981: The steady linear response of a spherical atmosphere to thermal and orographic forcing. *J. Atmos. Sci.,* **38,** 1179–1196.

Kimoto, M., F. F. Jin, M. Watanabe, and N. Yasutomi, 2001: Zonal-eddy coupling and a neutral mode theory for the Arctic Oscillation. *Geophys. Res. Lett.*, **28,** 737–740.

Kucharski, F., and F. Molteni, 2003: On nonlinearities in a forced NAO. *Climate Dyn.,* in press.

Kushnir, Y., and N.-C. Lau, 1992: The general circulation model response to a North Pacific SST anomaly: Dependence on time scale and pattern polarity. *J. Climate,* **5,** 271–283.

——, and I. M. Held, 1996: Equilibrium atmospheric response to North Atlantic SST anomalies. *J. Climate,* **9,** 1208–1220.

——, W. A. Robinson, I. Blade, N. M. J. Hall, S. Peng, and R. Sutton, 2002: Atmospheric GCM response to extratropical SST anomalies: Synthesis and evaluation. *J. Climate,* **15,** 2233–2256.

Latif, M., and T. P. Barnett, 1994: Causes of decadal climate vari-

ability over the North Pacific and North America. *Science,* **266,** 634–637.
Lau, N.-C., and M. J. Nath, 1991: Variability of the baroclinic and barotropic transient eddy forcing associated with monthly changes in the midlatitude storm tracks. *J. Atmos. Sci.,* **48,** 2589–2613.
Lin, H., and J. Derome, 2003: Atmospheric response to SST anomalies in the North Atlantic. *Tellus,* in press.
Marshall, J., H. Johnson, and J. Goodman, 2001a: A study of the interaction of the North Atlantic oscillation with ocean circulation. *J. Climate,* **14,** 1399–1421.
——, and Coauthors, 2001b: North Atlantic climate variability: Phenomena, impacts and mechanisms. *Int. J. Climatol.,* **21,** 1863–1898.
Palmer, T. N., and Z. Sun, 1985: A modeling and observational study of the relationship between sea surface temperature in the northwest Atlantic and atmospheric general circulation. *Quart. J. Roy. Meteor. Soc.,* **111,** 947–975.
Peng, S., and J. S. Whitaker, 1999: Mechanisms determining the atmospheric response to midlatitude SST anomalies. *J. Climate,* **12,** 1393–1408.
——, and W. A. Robinson, 2001: Relationships between atmospheric internal variability and the responses to an extratropical SST anomaly. *J. Climate,* **14,** 2943–2959.
——, L. A. Mysak, H. Ritchie, J. Derome, and B. Dugas, 1995: The differences between early and midwinter atmospheric response to sea surface temperature anomalies in the northwest Atlantic. *J. Climate,* **8,** 137–157.
——, W. A. Robinson, and M. P. Hoerling, 1997: The modeled atmospheric response to midlatitude SST anomalies and its dependence on background circulation states. *J. Climate,* **10,** 971–987.
——, W. A. Robinson, and S. Li, 2002: North Atlantic SST forcing of the NAO and relationships with intrinsic hemispheric variability. *Geophys. Res. Lett.,* **29,** 1276, doi:10.1029.2001GL014043.
Press, W. H., S. A. Teukolsky, W. T. Vetterling, and B. P. Flannery, 1994: *Numerical Recipes.* 2d ed. Cambridge University Press, 963 pp.
Robinson, W. A., 2000: Review of WETS—The workshop on extratropical SST anomalies. *Bull. Amer. Meteor. Soc.,* **81,** 567–577.
Rodwell, M. J., D. P. Rowell, and C. K. Folland, 1999: Oceanic forcing of the wintertime North Atlantic Oscillation and European climate. *Nature,* **398,** 320–323.
Sutton, R. T., W. A. Norton, and S. P. Jewson, 2000: The North Atlantic Oscillation—What role for the ocean? *Atmos. Sci. Lett.,* **1,** 89–100.
Thompson, D. W. J., and J. M. Wallace, 1998: The Arctic Oscillation signature in the wintertime geopotential height and temperature fields. *Geophys. Res. Lett.,* **25,** 1297–1300.
Ting, M., and N.-C. Lau, 1993: A diagnostic and modeling study of the monthly mean wintertime anomalies appearing in a 100-year GCM experiment. *J. Atmos. Sci.,* **50,** 2845–2867.
——, and M. P. Hoerling, 1993: Dynamics of stationary wave anomalies during the 1986/87 El Nino. *Climate Dyn.,* **9,** 147–164.
——, and S. Peng, 1995: Dynamics of the early and middle winter atmospheric responses to the northwest Atlantic SST anomalies. *J. Climate,* **8,** 2239–2254.
Wallace, J. M., C. Smith, and Q. Jiang, 1990: Spatial patterns of atmosphere–ocean interaction in the northern winter. *J. Climate,* **3,** 990–998.
Walter, K., U. Luksch, and K. Fraedrich, 2001: A response climatology of idealized midlatitude thermal forcing experiments with and without a storm track. *J. Climate,* **14,** 467–484.
Watanabe, M., and M. Kimoto, 2000: Atmosphere–ocean thermal coupling in the North Atlantic: A positive feedback. *Quart. J. Roy. Meteor. Soc.,* **126,** 3343–3369.
Whitaker, J. S., and P. D. Sardeshmukh, 1998: A linear theory of extratropical synoptic eddy statistics. *J. Atmos. Sci.,* **55,** 237–258.